

Electrical Conductivity and Structural characterization of Unhydrated 4-dimethylaminobenzylidenemalononitrile

G. F. Salem^a, E.A.A. El-Shazly^a, N. A. Elsayed^a, Magdy A. Ibrahim^b, K.F. Abd El-Rahman^a

^a Department of Physics, Faculty of Education, Ain Shams University, Rorxy, Cairo 11757, Egypt

^b Department of Chemistry, Faculty of Education, Ain Shams University, Rorxy, Cairo 11757, Egypt

*Corresponding author: E-mail address: karamelrahmen@edu.asu.edu.eg; Tel.: +201147579071

Abstract:

X-ray diffraction (XRD) patterns revealed that the powder material of 4-dimethylaminobenzylidenemalononitrile (DBM) has a polycrystalline structure. The analysis indicated that DBM molecule has monoclinic crystal structure with lattice parameters of $a = 16.992\text{nm}$, $b = 3.910\text{nm}$, $c = 9.391\text{nm}$, $\alpha = 90.00^\circ$, $\beta = 123.72^\circ$ and $\gamma = 90.00^\circ$. Thermal evaporation was used to prepare the thin films of DBM and led to crystalline films with preferred orientation to (520) plane. The calculations of XRD of as-deposited DBM thin film shows a nanocrystalline structure with crystallite size ranging from 59.22 nm to 71.94 nm. The crystallite size slightly increases with increasing film thickness and with increasing annealing temperatures of the films. The temperature dependence of electrical resistivity of DBM films showed that the dark electrical resistivity decreases as temperature of film increase and there are two conduction mechanisms through a thermally activated process. The average values of activation energies are $\Delta E_1 = 0.34\text{ eV}$ and $\Delta E_2 = 1.19\text{ eV}$ for extrinsic and intrinsic conduction mechanisms, respectively. The extrinsic to intrinsic conduction was attributed to the effect of ambient gases on the material.

Keywords: organic compounds; DC conductivity; structural.

1. Introduction

Organic semiconductors are recently in the spotlight because they are less expensive, lighter, and more flexible in shaping and manufacture when compared to silicon-based devices. Organic materials are based on conjugated small organic molecules and polymers. The search for new material with good performance characteristics as well as the improvement in device fabrication has been also a subject of interest. Organic semiconductors are used in a range of applications such as photographic sensitizer, light emitting diodes (OLEDs), field effect transistors (OFET) and solar cells (OSC). Donor–acceptor (D–A) chromophores are an important type of dyes that uses in potential applications such as photographic sensitizer [1] and optoelectronics devices [2]. An example of these dyes, 4-dimethylaminobenzylidenemalononitrile (DBM) is a disubstituted benzenes dye of the type donorphenyl-acceptor (D-ph-A) with a donor part (dimethylamino group) and a acceptor part (malononitrile group), where The molecular structure of DBM is obtained in Fig. 1. This dye is classified as molecular rotors [3], which have great importance as fluorescence probes of the flexibility of surrounding media [4], photoconductive recording materials [5] and It is used as sublimable dye in heat-transfer recording materials [6]. The delocalized π -electrons, the presence of functional groups, adsorbed species and defect sites is responsible for electrical conductivity of organic compounds [7]. Organic applications include gas sensors because the electronic transport properties of organic compounds are sensitive to adsorption of selective gases [8–11]. Moreover, there is an attraction to organic compounds due to their high dipole moments and strong intermolecular charge-transfer bands are at the origin of their first molecular hyperpolarizabilities and because of their second-order nonlinear optical response [12,13].

This research shows the structural properties of newly synthesized organic compound (DBM) [14,15] in powder form and thin film conditions, and the effects of film thickness and annealing temperatures on its structural properties. Moreover, the influence of surface states and gas adsorption on its electrical conductivity has been obtained. To the best of our knowledge, very few experimental researches were published on the structural and electrical properties of DBM.

2. Experiment technique

2.1 Material preparation

DBM is synthesized by the reaction between 4-dimethylaminobenzaldehyde (2.989 g, 20 mmol) and malononitrile (1.329 g, 20 mmol) in absolute ethanol (20 ml) containing few

drops of triethylamine was heated under reflux for 30 min. the yellowish orange crystals formed was filtered off and crystallized from ethanol. The melting point of the prepared material was determined to be 162°C.

2.2 Thin films preparation and used techniques

The deposition of thin films on substrate is achieved by using thermal evaporation technique, using high vacuum coating unit of 10^{-5} Pa (Edwards, E306A, UK). The material was heated up by passing a suitable current through the titanium evaporator. The deposition rate at 5 nms^{-1} and the thickness of the evaporated films were controlled using a quartz crystal thickness monitor. A group of samples of different thickness (130, 250, 480, and 590 nm) was prepared. To achieve a homogeneous film thickness, the substrates were mounted on a half-sphere holder. The structural properties of the films were examined by X-ray diffraction (XRD), scanning electron microscope (SEM) and Fourier Transform Infrared (FTIR). The scanning electron microscope (SEM) (JEOL JSM-T200) [16] was applied to the morphology of the film surface and to check the thickness of the evaporated films. The glass substrates have been cleaned sequentially according to the following steps: immersion in chromic acid for 24 h; followed by washing several times with distilled water, rinsing by ethyl alcohol, drying with dry air.

The heat treatment cycle of the DBM thin was carried out by heating the samples in air at 323, 373 and 423 K for 2 h and the samples were then cooled down to the room temperature inside the furnace.

XRD patterns of DBM in powder form, as deposited different thickness and annealed thin films were obtained by XRD system (Philips X' pert MPD) with Cu $K\alpha$ radiation ($\lambda = 0.15408 \text{ nm}$), operated at 40 KV and 30 mA. The diffractometer recorded the diffraction patterns automatically with a scanning speed of 2 degrees per minute. However, for determination of the crystallite size of the as deposited and annealed films the scanning speed for individual peaks was 0.5 degree per minute.

DBM is a p-type semiconductor that is investigated by hot probe method [17,18]. For the electrical measurements, the ohmic contacts were made by evaporating high purity Au through masks on the films at a vacuum of 10^{-5} Pa and checked by I-V characteristics at several values of temperature. A high impedance electrometer (Keithley, Model 610) measures the electrical resistance of DBM films with changing temperature by the two-probe method. The film resistivity (ρ) was calculated by the well-known equation:

$$\rho = R \frac{A}{L} = \sigma \quad (1)$$

where A is the cross-sectional area of the film, L is its length, R is its resistance and its dark electrical conductivity is (σ). The temperature was measured by NiCr-NiAl thermocouple monitored by a micro-voltmeter with powered by a stabilized dc power supply. We get that the dark electrical resistivity (σ) as a function of temperature.

3. Results and discussions

3.1 Structural characterizations

The FTIR spectrum for DBM powder is used to identify the functional groups and the molecular structure by absorbing IR radiation that causes the various bands in a molecule to stretch and bend with respect to one another. The IR spectrum contains two regions: fingerprint region, which is unique region for a molecule and the functional group region, which contains the peaks corresponding to the different functional groups. Figure 2. shows FTIR spectra of powder and all the wavenumber values of peaks values are listed in Table 1. There is not a broad intensity band, indicating to the absence of a hydroxyl group O-H. Therefore, the DBM powder under study is unhydrated. During the carrying out of all our measurements, we kept the samples away from the humidity by keeping them in a desiccator containing a strong hygroscopic material. A sharp absorption band appearing at 2210 cm^{-1} is referred to the stretching vibration of $\text{C}\equiv\text{N}$ group that forms conjugated bond with benzene ring.

Figure 3 represents the XRD patterns for the powder of DBM compound in powder form. It shows that the powder of DBM is in a polycrystalline nature.

By using the computer software, CRYSFIRE, and CHECKCELL for the powder form of DBM, the Lattice parameters of DBM were estimated [19, 20], see table (1). The calculation and analysis suggest that the DBM compound in powder form has a monoclinic crystal system with space group P^{21} and its lattice parameters were found to be $\mathbf{a} = 16.992\text{nm}$, $\mathbf{b} = 3.910\text{nm}$, $\mathbf{c} = 9.391\text{nm}$, $\mathbf{\alpha} = 90.00^\circ$, $\mathbf{\beta} = 123.72^\circ$ and $\mathbf{\gamma} = 90.00^\circ$. The major peak in XRD patterns for the DBM powder is observed at about ($2\theta = 11.231^\circ$) and its interplanar spacing is 7.87234 nm, which corresponds to reflection from (210).

Figure 4 represents the XRD patterns for the as-deposited DBM thin films for different thicknesses of 130, 250, 480, 590 nm. The films are crystalline and preferred oriented to the plane of (520). It is observed that the peaks start to appear at relatively thickness higher than

130 nm. It is also shown that the intensity of the preferred peak increases with increasing the film thickness. This indicated that the degree of crystallinity increases with increasing the of the film thickness. The crystallite size for each thickness was calculated by using by the Scherrer formula [21,22] as:

$$L = \frac{K_s \lambda}{\beta \cos \theta} \quad (2)$$

where λ is the X-ray wavelength of Cu K_α (0.1542 nm), and K_s is the Scherrer's constant, which is in order of unity (~ 0.95 [22]), β is a parameter in radian which can be obtained from the peak and corresponding to the half maximum intensity is the full-width at half maximum (FWHM), of the Bragg peak, and θ is the corresponding Bragg diffraction angle

The films have nanocrystallite structure with crystallite size 59.22, 65.77, 71.944 nm, respectively and the 2θ corresponding the peak are 26.757° , 26.777° , 26.777° , respectively. During the film preparation, the growth of crystals is preferred oriented. The position of the diffraction peak did not change by increasing the film thickness, however the nanocrystallite size slightly. The same results were also observed with the scanning electron microscope (SEM).

The dislocation density (δ), which is the number of dislocation lines per unit area of the film is given by [23]:

$$\delta = \frac{1}{L^2} \quad (4)$$

The grain size of the deposited films was calculated using Scherrer's formula. The variation of the crystallite size and dislocation density with film thickness for as-deposited DBM films is shown in figure 5.

Figure 6 presents XRD patterns of the as deposited and annealed DBM film of thickness 590 nm. As the annealing temperature of film increases, the intensity of diffraction peak increases and the crystallite size increases.

The grain size of the deposited films increased when the annealing temperature increased. The nanocrystallite of the film increased from 59.22 nm to be 63.16 and 65.77 when the sample was annealed at 50 and 100oC respectively for two hours. It was shown also that dislocation density decreased after annealing. The variation of the crystallite size and dislocation density with film thickness for as-deposited DBM films is shown in figure 7.

It is noticeable from this figure that as film thickness increases the crystallite size increases in nanoscale range, the full width at half maximum (FWHM) decrease and the dislocation density decreases non-linearly because of the release of internal stresses in the films as the gradual reduction in the stacking fault of the layers [24].

3.2 DC conductivity measurements

The electrical properties of DBM thin films were investigated. Electrical conductivity was measured for thin films in air. The temperature dependence of the electrical resistivities for DBM thin films were studied in the temperature range from 303 to 413 K. Figure 8 illustrates the effect of the temperature dependence of the dark electrical resistivity in the temperature range from 303 to 413 K for four films of different thicknesses.

Figure 8 illustrates the variation of dark electrical resistivity as a function of temperature for DBM films with different film thicknesses. Electrical resistivity decreases as the sample temperature increases indicating the semiconductor behavior of DBM films. This variation of resistivity with temperature means that the conduction is through a thermally activated process having two conduction levels (region 1 and region 2), see the figure. It is good to note that the value of resistivity is slightly varied with the thickness. This is because of thin film growth, where the small thickness contains a lot of islands which decrease by increasing the film thickness to reach the thick film. Obtaining of linear variation indicated that the results can be discussed by Arrhenius equation [25].

$$\rho = \rho_{01} \exp (\Delta E_1 / k_B T) + \rho_{02} \exp (\Delta E_2 / k_B T) \quad (5)$$

where ρ_{01} and ρ_{02} are the pre-exponential factors, ΔE_1 and ΔE_2 are the electrical activation energies in regions (1) and (2) respectively and k_B is the Boltzmann constant. From the slope we can estimate the activation energies and from the intercept we can get the resistivity pre-exponential factors. slopes of two regions were found to be nearly independent of film thickness, where the calculated activation energies were found to be close to each other's. The average values of activation energies were found to be $\Delta E_1 = 0.34$ eV and $\Delta E_2 = 1.19$ eV. This leads us to suggest that the first region is due to extrinsic behaviour and the second region is due to intrinsic behaviour. It can be suggested that the extrinsic behaviour could be due to the introducing of an external impurity such as gases or water vapor which can be adsorbed on the sample surface [26]. This suggestion was verified by measuring the electrical conduction through the sample in both air and vacuum. The conduction in air was found to be higher than that measured in vacuum. This behaviour is a normal case for most organic semiconductor due to their high sensitivity to the presence of various gases in the ambient atmosphere [27]. This

means that presence of gases and water vapour molecules in the material improve the conductivity where they act as acceptor dopants. The effect of the ambient gases on the conduction was also checked by measuring the resistivity measurements of a thin film sample through heating cooling regime. Figure 9 shows the resistivity measurements for DBM thin film through three heating/cooling runs (heating, cooling, and heating back runs). It was found that the first heating run includes two different regions with two different activation energies indicating that the conduction of the DBM is affected by the gases present on the sample. The ambient gases in this case act as external impurity dopant. When the temperature of the sample reaches a certain temperature, gases and water vapour start to leave the material until it becomes undoped semiconductor. Hence, the conduction of the material is carried out through intrinsic conduction. As observed in figure 9, an activation energy nearly equal to the intrinsic one is obtained over the whole range. This indicates that the gases and water vapor, which were removed during the first heating run, will take time to be totally adsorbed again on the sample. This means that the disappearance of extrinsic behavior in the cooling and the second heating runs could be explained, as the rate adsorption of all the gases and water molecules is not enough to back the material to extrinsic again.

4. Conclusions

4-dimethylaminobenzylidenemalononitrile, DBM, was synthesized by the reaction between 4-dimethylaminobenzaldehyde and malononitrile in absolute ethanol containing few drops of triethylamine was heated under reflux for 30 min. Yellowish orange crystals were obtained with melting point of 162°C. X-ray diffraction pattern (XRD) of DBM in powder form showed that it has a polycrystalline form with monoclinic system. Thermal evaporation of DBM led to crystalline films with preferred orientation to (520) plane. The obtained films have nanocrystallite structure and the crystallite size increases with increasing the film thickness and the annealing temperature. The dark electrical resistivity measurements showed semiconductor behaviour with two activation energies. The change in the activation energy is interpreted as a change from extrinsic to intrinsic conduction due to the effect of ambient gases.

References

1. H. Ringsdorf, L. Cabres, A. Dittrich, *Ang. Chem. Int. Ed.* 30, 76 (1991)
2. D.J. Willhams, *Ang. Chem. Int. Ed.* 23, 690 (1984)
3. R.O. Loutfy, K.Y. Law, *J. Phys. Chem.* 84 (1980) 2803e2808.
4. R.O. Loutfy, B.A. Arnold, *J. Phys. Chem.* 86 (1982) 4205e4211.

5. R.O. Loutfy, Pure Appl. Chem. 85 (1986) 1239e1248.
6. K.Y. Law, Chem. Phys. Lett. 75 (1980) 545e549.
7. P.G. Collins, K. Bradley, M. Ishigami, A. Zettl, Science 287, 1801 (2000)
8. A.M. Saleh, R.D. Gould, A.K. Hassan, Phys. Status Solidi. A 139, 334 (1993)
9. R.A. Collins, K.A. Mohammed, Thin Solid Films 145, 133 (1986)
10. M. Sakaguchi, M. Ohta, J. Solid State Chem. 61, 130 (1986)
11. B. Schollhorn, J.P. Germain, A. Pauly, C. Maleysson, J.P. Blanc, Thin Solid Films 326, 245 (1986)
12. H.S. Miyata, Nonlinear Optics of Organic Molecules and Polymers (CRC Press, Boca Raton, 1997)
13. J.J. Wolf, R. Wortmann, Adv. Phys. Org. Chem. 32, 12 (1999)
14. A.M. Asiri, J. Saudi Chem. Soc. 6, 51 (2002)
15. M.M. El-Nahass, H.M. Zeyada, K.F. Abd El-Rahman, A.A.M. Farag, A.A.A. Darwish, Spectrochimica Acta Part A 69, 205 (2008)
16. S. Tolansky, Multiple – Beam Interference Microscopy of Metals (Academic Press, London, 1970)
17. D.K. Schroder, Semiconductor Material and Device Characterization (John Wiley & Sons, Inc., New York, 1998)
18. Keithley Instruments, Inc., Low Level Measurements Handbook, 6th edn. (Keithley Instruments, Inc., Cleveland, Ohio, 2004)
19. R. Shirley, The CRYSFIRE System for Automatic Powder Indexing: User's Manual (The Lattice Press, Guildford, England, 2000)
20. J. Laugier, B. Bochu, LMGP-Suite suite of Programs for the Interpretation of X-ray Experiments, ENSP/Laboratoire des Matériaux et du Génie Physique (Saint-Martin-d'Hères, France, 2000)
21. V. Holý, U. Pietsch, T. Baumbach, High Resolution X-ray Scattering From Thin Films and Multilayers (Springer, Berlin, 1999)
22. A.K. Hassan, R.D. Gould, Phys. Status Solidi A 132, 91 (1992)
23. S. Velumani, X. Mathew, P.J. Sebastian, Solar Energy Mater. Solar Cells 76, 359 (2003)
24. T. Mahalingam, S. Thanikaikarasan, R. Chandramohan, M. Raja, C. Sanjeeviraja, J.-H. Kim, Y.D. Kim, J. Mater. Chem. Phys. 106, 369 (2007) 32. B.A.
25. B.A. El-Sayed, M.M. Sallam, M.F. Ishak, M.S. Antonious, Materials Letters 34 (1998) 280
26. M.M. El-Nahass, H.M. Zeyada, K.F. Abd-El-Rahman, A.A.A. Darwish, Applied Surface Science 253 (2007) 8597-8601
27. M. Pope, C.E. Swenberg, Electronic Processes in Organic Crystals and Polymers, 2nd edn. (Oxford University Press, Oxford, 1999)

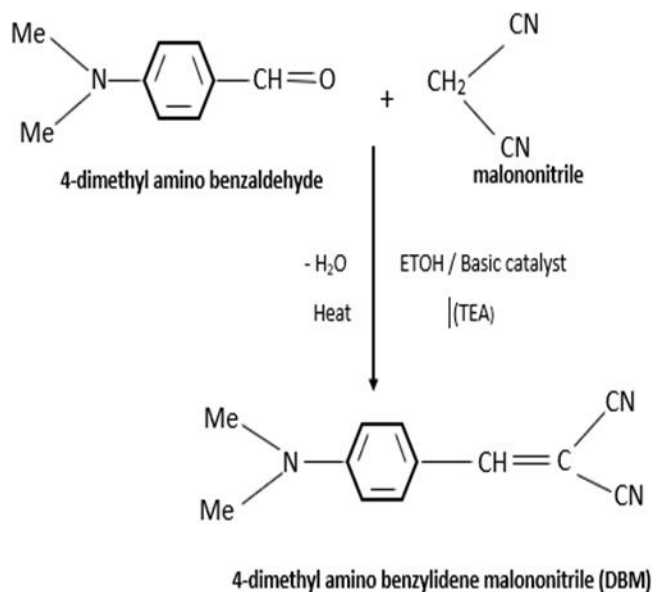


Figure 1. The chemical reaction of the DBM compound

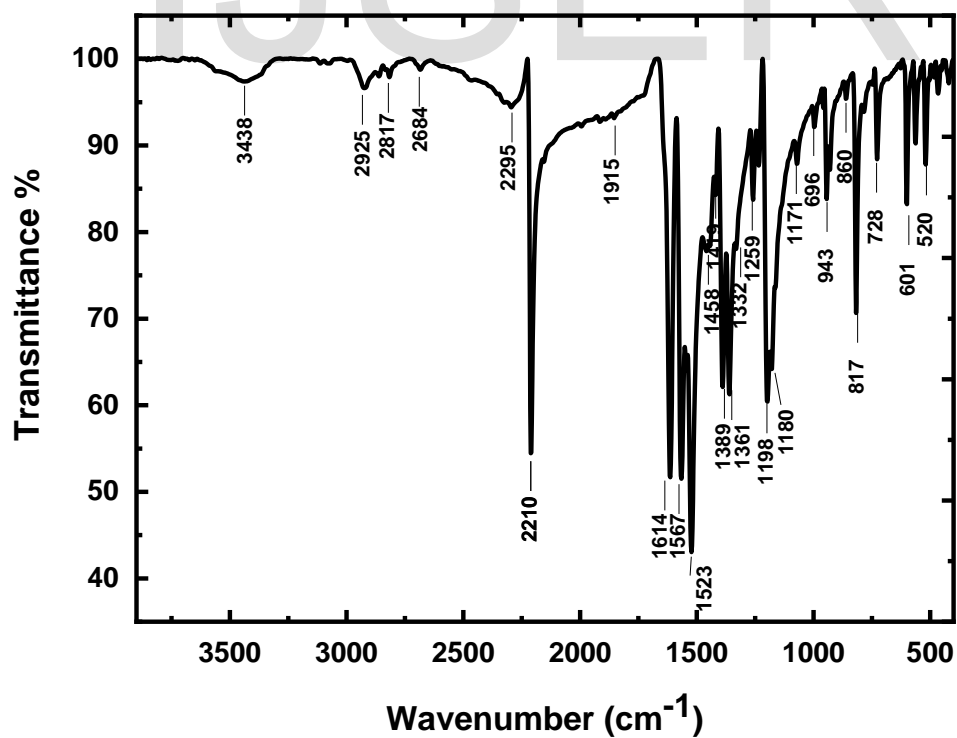


Figure. 2. The experimental FT-IR spectrum of DBM molecule in powder form

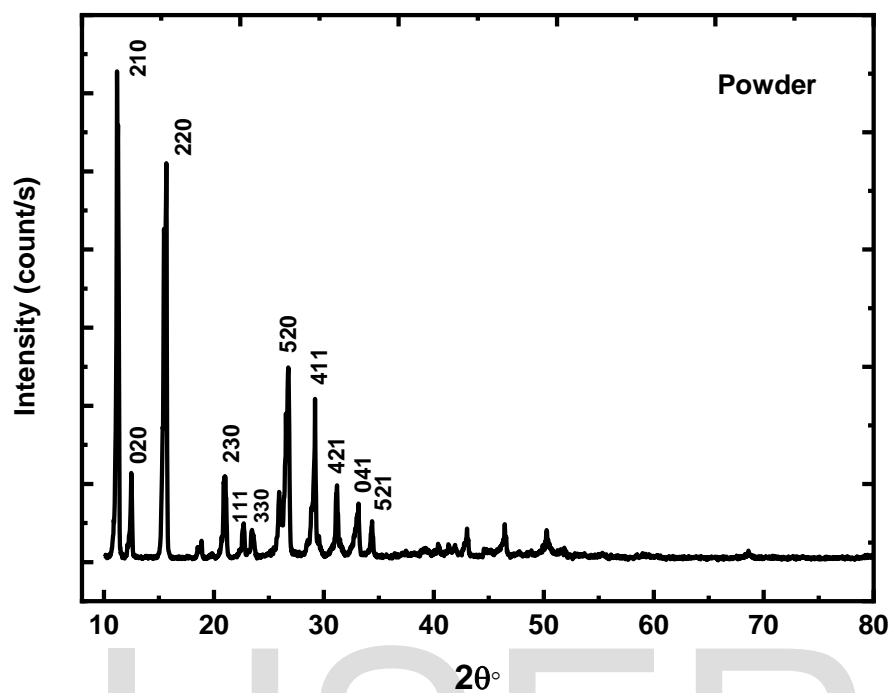


Figure 3 X-ray diffraction of DBM compound in the powder form.

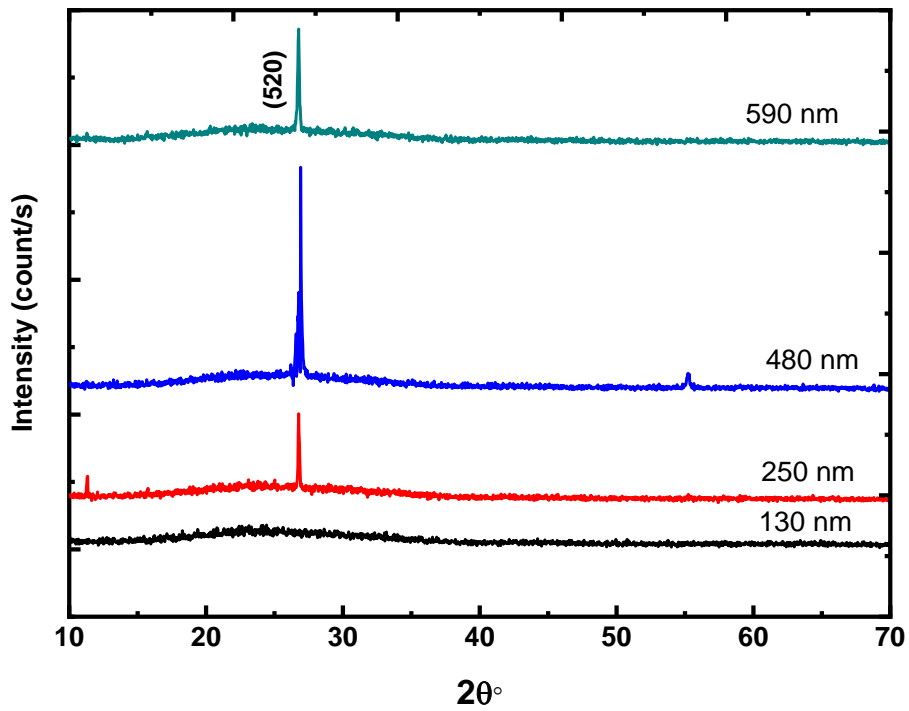


Figure 4: X-rays diffraction patterns for as-deposited TCVA films of different thicknesses

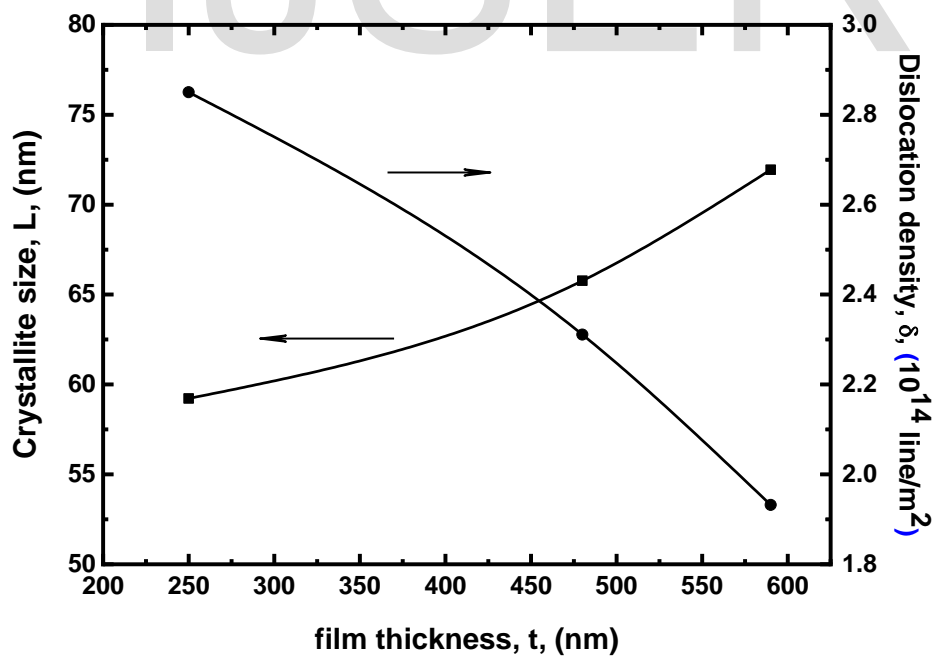


Figure 5 The mean crystallite size, L , and dislocation density, δ , as a function of the film thickness, d

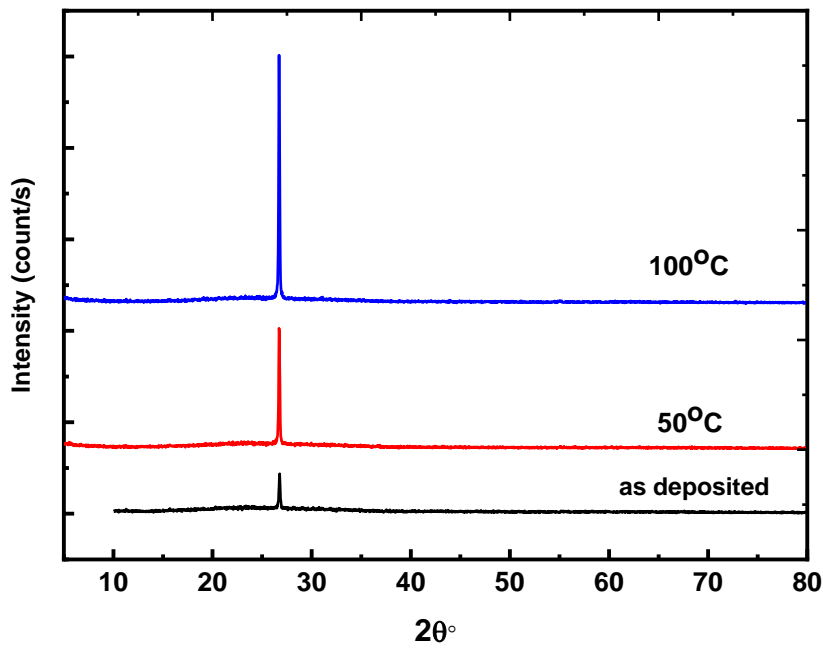


Figure 6. X-ray diffraction patterns for as deposited and annealed DBM films of thickness 590 nm

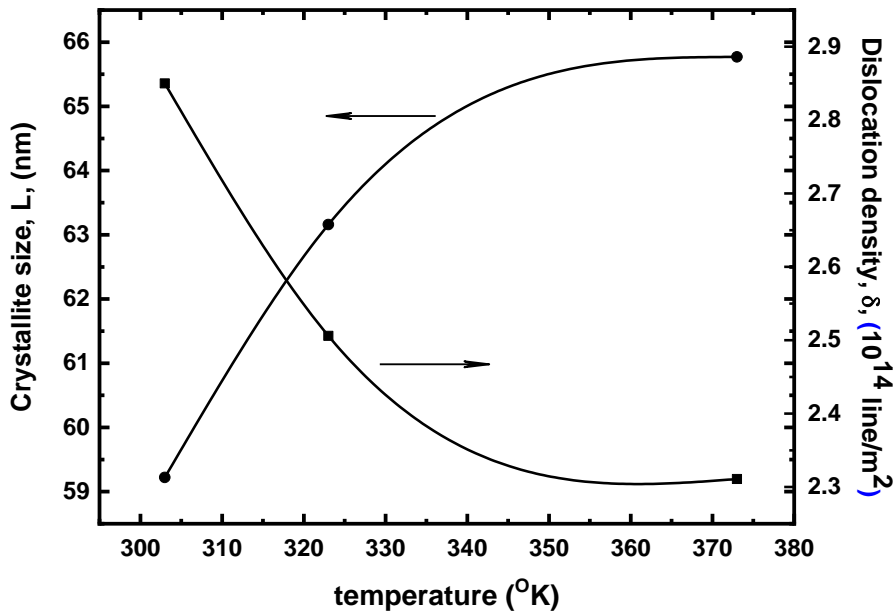


Figure 7 The values of the crystallite size (L), and dislocation density (δ) of as-deposited and annealed DBM films with the temperature

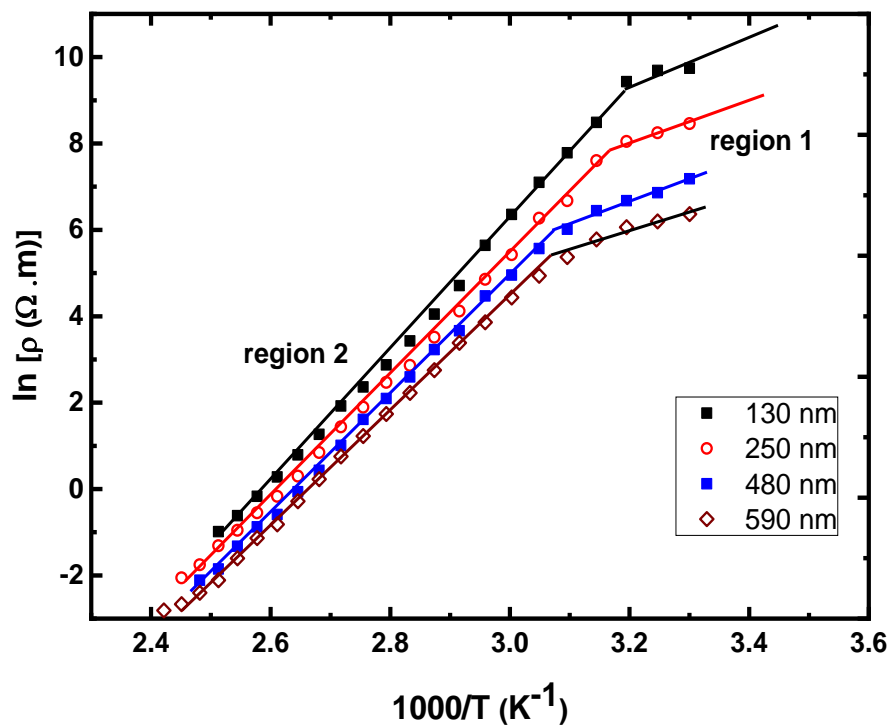


Figure 8 Temperature dependence of electrical resistivity of DBM thin films with different thicknesses.

IJSER

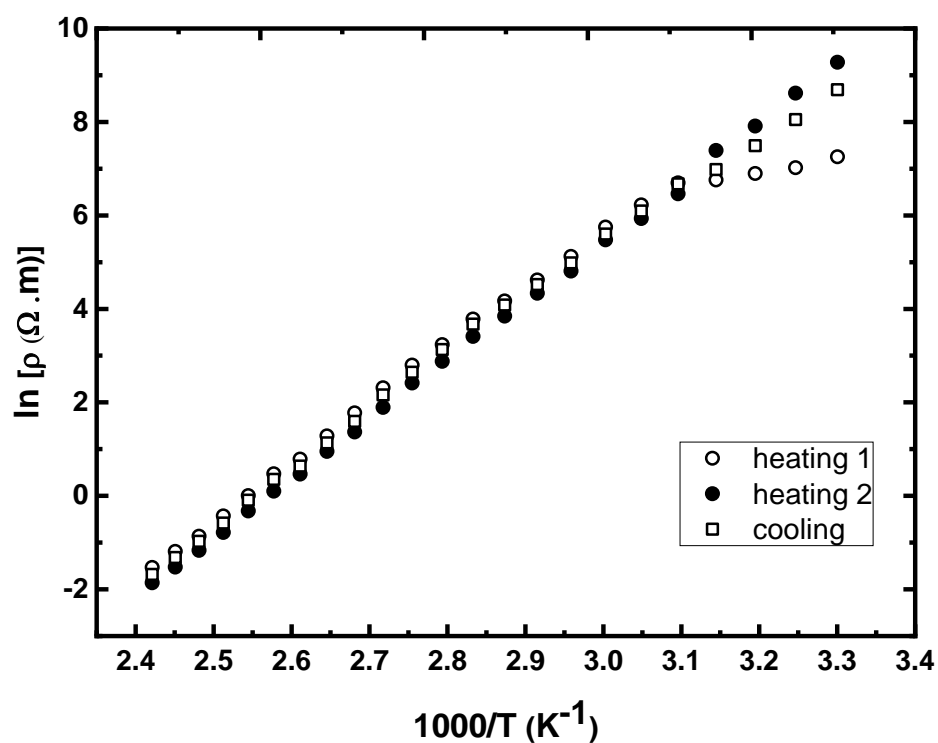


Figure 9: Temperature dependence of the electrical resistivity of DBM thin film through heating-cooling-heating regime

| Frequency (cm ⁻¹) | Absorption band |
|-------------------------------|-----------------|
|-------------------------------|-----------------|

| | |
|-----------|---------------------------------|
| 2925 | ν (C–H) stretching |
| 2210 | ν (C \equiv N) stretching |
| 1614 | ν (C=C) stretching |
| 1567 | ν (C=C) aromatic stretching |
| 1523 | ν (C–H) bending |
| 1361 | ν (C–H) methyl bending |
| 1198-1180 | ν (C–N) stretching |
| 943 | ν (C=C) |
| 817 | ν (C–H) aromatic |
| 728 | ν (C–H) aromatic |
| 601 | ν (C–H) aromatic |

Table 1: The position of band in FTIR spectra of DBM powder

IJSER